Cardiovascular Engineering and Technology, Vol. 10, No. 2, June 2019 *(© 2019)* pp. 242–256
https://doi.org/10.1007/s13239-019-00400-x

MRI and Blood Flow in Human Arteries: Are There Any Adverse Effects?

K. GAYATHRI and K. SHAILENDHRA

Department of Mathematics, Amrita School of Engineering, Coimbatore, Amrita Vishwa Vidyapeetham, Coimbatore 641 112, India

(Received 28 December 2016; accepted 7 January 2019; published online 28 January 2019)

Associate Editors Dr. Ajit P. Yoganathan and Dr. Mark Fogel oversaw the review of this article.

Abstract

Purpose—To explore if there are any adverse effects on blood flow in human beings when they are exposed to high or ultra high intensity magnetic fields in MRI, by investigating both qualitatively and quantitatively the effects of such fields on the velocity of blood and medically significant hemodynamic wall parameters such as wall shear stress (WSS), oscillatory shear index (OSI) and relative residence time (RRT) in four human large arteries.

Methods—Blood flow in an artery is approximated as a flow through a uniform circular tube with rigid porous walls and the well-known McDonalds model is employed by using pressure gradient waveforms reported in the medical literature.

Results—No significant change in the above parameters is observed up to 3*T* in all these arteries except a discernible change in the velocity and RRT in the pulmonary artery. Very significant changes are noticed in the above parameters beyond 8T in the pulmonary artery. The common hypothesis that low WSS and high OSI co-locate is not acceptable.

Conclusions—Our results suggest that the clinical consequences are to be carefully considered before exposing human beings to ultra high field MRI. It may not be appropriate to conclude anything about the effect of magnetic field on blood flow in human beings based on experimental studies on animals, which is one of the reasons for the contradicting reports found in the literature. A slip condition at the wall which is appropriate to hemodynamics is yet to be developed.

Keywords—High intensity static magnetic field, Hemodynamic wall parameters, Wall shear stress, Oscillatory shear index, Relative residence time, Interface condition.

INTRODUCTION

The idea of employing electromagnetic fields in the medical research was conceived initially by Kolin[22] in the year 1936. He established that the biological systems in general are greatly affected by the application of external magnetic field. Barnothy[2] noticed a significant decrease in the heart rate by exposing biological systems to an external magnetic field. The possibility of regulating the blood flow movement in human system by applying external magnetic field was discussed as early as 1965 by Korchevskii and Marcochnik.[23] However, it was only during 1980s' engineers got attracted towards the application of a magnetic field in biomedical engineering, primarily with an intention of utilizing magnetohydrodynamic (MHD) principles, in controlling blood flow velocities in surgical procedures and also in understanding and establishing the effects of magnetic fields on blood flows in astronauts and citizens living in the vicinity of electromagnetic towers.[27]

Over the past few decades, extensive research work has been carried out that involves the flow of electrically conducting fluids in the presence of high intensity magnetic fields (high intensity MHD) in many scientific disciplines, including medicine, chemistry, condensed matter physics, plasma physics and high energy physics owing to its numerous applications ranging from studying brain functionality to high temperature superconductivity.[6] During this period, with the invention of new and powerful magnetic materials and equipment, many medical diagnostic devices, especially those used in diagnosing Cardio Vascular Diseases (CVDs) and neurological disorders, started making use of high intensity Static Magnetic Fields (SMF). For example, in medical sciences, it is used for reduction of bleeding during surgeries, provocation of occlusions of the feeding vessels of cancer tumor and for targeted

Address correspondence to K. Shailendhra, Department of Mathematics, Amrita School of Engineering, Coimbatore, Amrita Vishwa Vidyapeetham, Coimbatore 641 112, India. Electronic mail: k_gayathri@cb.amrita.edu, k_shailendhra@cb.amrita.edu, shailendhrak@gmail.com

1869-408X/19/0600-0242/0 © 2019 Biomedical Engineering Society

drug delivery with relatively high accuracy. In bioengineering, it is used to investigate the blood flow through an artery, peristaltic food motion in the intestine, motion of urine in urethra and design of prosthetic devices. Also, high intensity magnetic fields are employed in certain advanced laboratory studies in astrophysics, geophysics, terrestrial, solar plasma and nuclear magnetic resonance.[6] Kamil Ugurbil *et al.*[39] pointed out that the use of very high intensity magnetic fields such as 7Tesla (T) in human studies is still in its infancy even in the developed countries. Therefore, it is essential to investigate if there are any adverse effects when human beings are exposed to such high intensity magnetic fields employed in all the above mentioned advanced areas of research, and in particular Magnetic Resonance Imaging (MRI) systems, in order to develop and implement appropriate safety protocols.

MRI is a widely used medical imaging technique for medical diagnosis and prognosis of the diseases without exposing the body to radiation and it requires a powerful magnet of uniform and strong magnetic field strength. MRI scanners are broadly classified into closed bore and open bore scanners. In cylindrical/closed bore scanners the magnetic field is oriented along the head-feet direction, whereas in the open scanners it is oriented in a direction perpendicular to the head-feet direction of the patient.[7,17] In conventional MRI systems, the SMF strength employed is $1.5T$ and in 2002 the Food and Drug Administration (USA) has approved $3T$ MRI. The knowledge gained over the past two decades on the interaction of SMFs with the biological tissues has paved the way to increase the SMF strength from 0.1 to $8T$ in MRI systems. The basic reasons behind increasing the SMF strength in MRI are that (i) it results in high quality images due to high spatial resolution that is achieved as a result of increased Signal to Noise Ratio (ii) the dosage of contrast agents that are nephrotoxic can be considerably reduced and (iii) the acquisition time is also appreciably reduced which in turn reduces the motion artifacts.[16] For example, in the field of functional neuro imaging, $8T$ MR images provided new insights into stroke imaging and by demonstrating infarctions with unprecedented resolution and revealing lesions that were not apparent at $1.5T$ MRI.[29] For a complete account on the historical perspectives of MRI one may refer to Tal Geva[16] and for an excellent and comprehensive survey on the effects of magnetic field on blood flow and blood vessels in the microvasculature one may refer to McKay *et al.*[27]

The discussions regarding the safety issues and procedures associated with MRI systems have been extremely controversial over the past two decades as pointed out by Formica and Silvestri.[9] Further, they have highlighted that the possible reason for such a controversy is due to the unclear claims about the role of electromagnetic fields and the lack of authentic publications on negative results and possible potential hazards involved in using MRI systems.[9] Ultimately, Schenck[31] in his review article warned that it cannot be categorically concluded that there are no significant biological effects of SMF because of certain difficulties in documenting the negative results. In order to resolve the controversies, however, we cannot expose human beings to ultra high intensity SMF as there are inherent restraints and prohibitions. Thus, one of the possible ways to address these issues is to investigate the effects of high intensity SMFs on the blood flow in the arteries of human beings through an appropriate mathematical modeling which enables a clinician, medical or biological research worker to understand the complex phenomena associated with the pathophysiological mechanisms as well as the hemodynamics in disease free arteries. This motivated us to choose the physiological pressure gradient waveforms of arteries reported in the cardiology literature for various sites on the Cardio Vascular System (CVS) such as the arm (brachial), leg (femoral), heart muscles (coronary) and the pulmonary artery for studying the effects of SMF on the Hemodynamic Wall Parameters (HWPs) which are responsible for the pathogenesis of vascular diseases.

Thus, the present investigation is motivated on the basis of modern medical applications and demand for continuous research to study the possible clinical consequences on employing high, ultra high intensity MRI for the purpose of medical diagnosis and prognosis. This work is the direct extension of our recent work,[14] taking into account the Lorentz force due to an applied uniform transverse magnetic field of strength varying from 0 to $20T$. To the best of our knowledge, this is the very first exhaustive comparative study on the effects of high intensity SMF on the velocity of blood and the medically significant HWPs such as wall shear stress (WSS), oscillatory shear index (OSI) and relative residence time (RRT) in the large human arteries belonging to the coronary, systemic and pulmonary circulations. In order to make our article self-contained, we provide sufficient details on the physiological significance on HWPs in "Significance of Hemodynamic Wall Parameters (HWPs)". In addition, the results obtained with no slip condition at the lumen wall interface are compared with those using Saffman slip condition.

MATHEMATICAL FORMULATION AND SOLUTION

Consider the pulsatile motion of blood through an artery of uniform circular cross section under the influence of an externally applied uniform transverse

magnetic field. Let the z-axis be taken along the axis of the tube. The flow is assumed to be axisymmetric. Then, the basic equations in the cylindrical coordinates (r, θ, z) are :

$$\text{The equation of continuity} : \nabla \cdot \overline{q} = 0 \text{ where } \overline{q} = [u_r, u_\theta, u_z] = [0, 0, u] \text{ is the velocity vector.} \quad (1)$$

$$\text{The equation of motion} : \rho\left(\frac{\partial \overline{q}}{\partial t} + (\overline{q}.\nabla)\overline{q}\right) = -\nabla p + \mu\nabla^2\overline{q} + \overline{j} \times \overline{B}. \quad (2)$$

where ρ, μ, p and t denote the density, the viscosity, the pressure and time. $\overline{j}$ and $\overline{B}$ denote the current density and the magnetic induction vector.

The magnetic field of strength $\overline{B}_0$ is applied along either the x-axis or the y-axis (refer Fig. 1). By Ohm's law, $\overline{j} = \sigma[\overline{E} + \overline{q} \times \overline{B}]$ where σ denotes the electrical conductivity of blood. Since no external electric field $\overline{E}$ is applied, it follows that the Lorentz's force $\overline{J} \times \overline{B}$ is given by—$\sigma u B_0^2 \hat{e}_z$ in both the cases (refer Appendix 1). It must be noted here that $R_m \ll 1$, where R_m is the magnetic Reynolds number of blood and hence the induced magnetic field is neglected (refer Appendix 2). Hence, the equation of motion reduces to

$$\frac{\partial u}{\partial t} - \frac{\mu}{\rho}\left[\frac{\partial^2 u}{\partial r^2} + \frac{1}{r}\frac{\partial u}{\partial r}\right] + \frac{\sigma}{\rho}B_0^2 u = -\frac{1}{\rho}\frac{\partial p}{\partial z} \quad (3)$$

It has been established that blood can be treated as Newtonian whenever the radius of an artery is greater than 0.0025 m.[28] The radius of the arteries considered in the present study are greater than 0.0025 m and hence blood is considered to be Newtonian. Further, Shukla *et al.*[33] used several different non-Newtonian models for simulations of blood flow in large arteries and they observed that there is no effect of the yield stress of blood on either the velocity profiles or WSS.

The appropriate boundary conditions are

$$u \text{ is finite when } r = 0;\ u = u_B = 0 \text{ when } r = R \text{ (no slip condition)} \quad (4)$$

where R is the radius of the artery and u_B is the slip velocity at the wall.

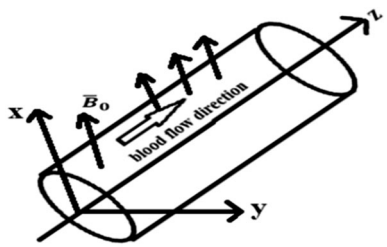

FIGURE 1. Schematic representation of blood flow.

The real challenge in carrying out hemodynamic study lies in the mathematical description of the axial pressure gradient in a cardiac cycle in a more realistic way. We have established in our earlier articles[13,14] that the McDonald's model is by far superior to any of the existing models in describing the pressure gradient. In this regard, one may refer to Chaturani and Bharatiya[4] and Nichols and O'Rourke[28] in addition to the above mentioned articles. The McDonald's model for pressure gradient is given by

$$-\frac{\partial p}{\partial z} = A_0 + \sum_{n=1}^{m}[A_n \cos(n\omega t) + B_n \sin(n\omega t)] = p_0 + Re\left[\sum_{n=1}^{m} p_n e^{i(n\omega t - \gamma_n)}\right] \quad (5)$$

where $p_0 = A_0$, $p_n = \sqrt{A_n^2 + B_n^2}$, $\gamma_n = arc\tan(B_n/A_n)$ and 'm' denotes the number of harmonics considered.

To ensure that our results are medically reliable, the pressure gradient waveforms of the coronary, brachial, femoral and pulmonary arteries available in the medical literature are utilized while mathematically describing the pressure gradient using the above McDonald's model.

Womersley and McDonald[28] in their classical and seminal work on the pulsatile blood flow categorically established, beyond any doubt, that the arterial system can be regarded as a linear system in steady state oscillation. Further, they also demonstrated that the nth harmonic of the velocity is influenced only by the nth harmonic of the pressure gradient and by no other harmonic. Hence, to find the analytical solution, pulsatile velocity in the lumen and the slip velocity at the lumen-wall interface caused by the pulsatile pressure gradient can be expressed as

$$u(r,t) = \overline{u}(r) + Re\sum_{n=1}^{m}\left[\tilde{u}_n(r)e^{i(n\omega t - \gamma_n)}\right] \quad (6)$$

$$u_B(t) = \overline{u}_B + Re\sum_{n=1}^{m}\left[\tilde{u}_{Bn}e^{i(n\omega t - \gamma_n)}\right] \quad (7)$$

The physical quantities are cast in the non dimensional form using the characteristic length R, the characteristic time ω^{-1} and the characteristic velocity $R\omega$. Thus, the non-dimensional equations for the steady part of the velocity $\overline{u}$ and the nth harmonic of the oscillatory part of the velocity $\overline{u}_n$ are given by

$$\frac{\partial^2 \overline{u}}{\partial r^2} + \frac{1}{r}\frac{\partial \overline{u}}{\partial r} - M^2\overline{u} = -\frac{p_0 R}{\mu\omega} \quad (8)$$

with boundary conditions for steady part given by $\overline{u}$ is finite, when $r = 0$; $\overline{u} = \overline{u}_B = 0$, when $r = 1$ and

$$\frac{\partial^2 \tilde{u}_n}{\partial r^2} + \frac{1}{r}\frac{\partial \tilde{u}_n}{\partial r} - \left[M^2 + in\left(\frac{R^2\omega\rho}{\mu}\right)\right] = -\frac{p_n R}{\mu\omega} \quad (9)$$

with the boundary conditions $\tilde{u}_n$ is finite, when $r = 0$; $\tilde{u}_n = \tilde{u}_{B_n} = 0$, when $r = 1$. Here, $M = \sqrt{\sigma_e B_0^2 R^2/\mu}$ denotes the Hartmann number, which is the ratio of the magnetic force to the viscous force and $\alpha = \sqrt{R^2\omega\rho/\mu}$ denotes the Womersley number, which is the ratio of the inertial force to the viscous force. The value of the Hartmann number for all the four arteries for various SMF strength is provided in Table 1.

The velocity of blood in the lumen of the artery is given by (details are provided in Appendix 3)

$$u(r,t) = \frac{p_0 R}{\mu\omega M^2}\left[1 - \frac{I_0(Mr)}{I_0(M)}\right] + Re\sum_{n=1}^{m}\left[\frac{p_n R}{\mu\omega(M^2 + in\alpha^2)}\left[1 - \frac{I_o(\sqrt{M^2 + in\alpha^2}r)}{I_o(\sqrt{M^2 + in\alpha^2})}\right]e^{i(n\omega t - \gamma_n)}\right] \quad (10)$$

where I_0 is the modified Bessel function of order zero.

SIGNIFICANCE OF HEMODYNAMIC WALL PARAMETERS (HWPS)

A thorough knowledge of the role of HWPs is essential for estimating the potential risks of vascular diseases or in predicting the natural history of atherosclerosis in large arteries. Hence, in this Section, we recollect not only the definitions of WSS, OSI and RRT, the medically significant trio of HWPs, but also provide the biological significance of these parameters in the formation and the development of plaque in arterial vasculature based on the reports available in the literature. It must be noted here that due to the applied magnetic field the velocity gets modified due to the Lorentz force. Owing to this, the three HWPs also get modified due to the applied field since these parameters essentially depend on the velocity.

Wall Shear Stress (WSS)

One of the main pathogenic factors in the development of atherosclerosis or aneurysm is WSS and is defined as

$$\tau = \mu\left(\frac{\partial u}{\partial r}\right)_{r=R} \quad (11)$$

In 1969, Fry[10] suggested that high WSS leads to endothelial damage and subsequent pathological responses. However, Caro *et al.*[3] proposed that high WSS is protective and that lesions are formed in the regions of low WSS. In fact, the spatial and temporal variations of arterial endothelial WSS are believed to influence the location of potential atherosclerotic plaque formation. The WSS is converted to biological signals by mechanoreceptors of endothelial cells, through a process called mechanotransduction, which in turn trigger various chemical reactions to modulate gene expressions and the cellular functions of the vessel wall that may be atheroprotective or may cause atherosclerosis or aneurysm.[8]The mechanical and biological significance of WSS is well explained in our earlier article.[14] For further details on the role of WSS in the regulation of blood vessel responses by the mechanotransduction mechanisms that lead to biophysical, biochemical and gene regulatory responses of endothelial cells one may refer to the review article by Davies[8] that covers almost all aspects in this regard.

Oscillatory Shear Index (OSI)

Not only the magnitude of WSS but also the temporal fluctuations in the direction of WSS vector also been identified as a key factor causing damage to the endothelial cells. To quantify this aspect, He and Ku [18] introduced an index called OSI as a marker of the oscillatory nature of WSS. It is a dimensionless measure of the directional changes in WSS over each cardiac cycle and is defined as

$$OSI = \frac{1}{2}\left[1 - \frac{I_1}{I_2}\right] \quad (12)$$

where $I_1 = \frac{1}{T}\left|\int_0^T \tau dt\right|, I_2 = \frac{1}{T}\int_0^T |\tau| dt$ and T is the pulse period, in seconds. That is, I_1 represents the time averaged absolute value of the total WSS and I_2 represents the time-average of the absolute values of the WSS, over a cardiac cycle. The value of OSI varies from 0 to 0.5 and it represents the fraction of the cardiac cycle over which the instantaneous shear force

TABLE 1. Hartmann number for various magnetic field strength.

Artery	0T	1.5T	3T	5T	8T	10T	20T
Coronary artery	0	0.0291	0.0581	0.0968	0.155	0.1937	0.3874
Brachial artery	0	0.0436	0.0872	0.1453	0.2324	0.2905	0.5811
Femoral artery	0	0.0639	0.1278	0.2131	0.3409	0.4261	0.8523
Pulmonary artery	0	0.2615	0.5230	0.8716	1.3946	1.7433	3.4866

TABLE 2. HWPs of coronary artery for various magnetic field strength.

Coronary artery-HWPs	0T	1.5T	3T	5T	8T	10T	20T
Mean velocity (m/s)	0.2073	0.2073	0.2072	0.2069	0.2064	0.2058	0.2016
% Change		− 0.02	− 0.06	− 0.18	− 0.45	− 0.70	− 2.74
Mean WSS (Pa)	− 1.1055	–	–	–	–	–	–
% Change		0.02	0.04	0.12	0.30	0.47	1.83
OSI	0.0864	0.0864	0.0865	0.0865	0.0867	0.0869	0.0882
% Change		0.01	0.05	0.13	0.34	0.53	2.06
RRT (N/m^2)	0.9049	0.9050	0.9053	0.9060	0.9076	0.9084	0.9179
% Change		0.01	0.04	0.12	0.30	0.39	1.44
Peak velocity (m/s)	0.5101	0.51	0.5099	0.5095	0.5086	0.5077	0.5006
% Change		− 0.0196	− 0.0392	− 0.1176	− 0.2941	− 0.4705	− 1.8624
Minimum velocity (m/s)	–	− 0.1444	− 0.1444	− 0.1443	0.1443	0.1443	0.144
% Change	–	0	0	− 0.0693	− 0.0693	− 0.0693	− 0.2770
Peak WSS (Pa)	0.9658	0.9658	0.9658	0.9658	0.9659	0.9660	0.9663
% Change	–	0	0	0	0.0104	0.0207	0.0518
Minimum WSS (Pa)	− 2.967	− 2.967	− 2.966	− 2.965	− 2.962	− 2.959	− 2.936
% Change	–	0	− 0.0337	− 0.0674	− 0.1685	− 0.2696	− 1.0448

vector forms an angle greater than 90° to the time averaged direction of the same force.

Relative Residence Time (RRT)

In 2004, Himburg *et al.*[19] reasoned that a combination of WSS and OSI reflects the residence time of the blood particles near the wall and introduced the notion of RRT as a marker of low or oscillatory WSS and defined it as

$$RRT \approx \left[(1 - 2 \times OSI)\left(\frac{1}{T}\int_0^T |\tau| dt\right)\right]^{-1} \qquad (13)$$

RRT is simply another type of Time Averaged WSS (TAWSS), but inverted and with a more tangible connection to the biological mechanisms underlying atherosclerosis.[25]

In this formulation, OSI acts to modify the effect of time-averaged shear on the RRT at a site. RRT prolongation corresponds to low or oscillatory WSS.[18] Obviously, when OSI is relatively small, its effect on RRT is not very significant. However, when OSI approaches its upper limit of 0.5, RRT increases substantially. Thus, in flows where OSI is relatively large, RRT is an useful measure of the shear environment for correlative purposes, which incorporates the combined effect of TAWSS and OSI.[25]

RESULTS AND DISCUSSIONS

It must be noted here that the results reported in this study are subject to the assumption that the applied magnetic field is either transverse (x-axis) or perpendicular (y-axis) to the direction of flow (z-axis) (refer Fig. 1). In order to make our results medically relevant, the parameter values used for computations in the present analysis are based on the data available in the cardiovascular literature: The density and viscosity of the blood are 1050 kg m^{-3} and 0.004 kg m^{-1} s^{-1} respectively. The radius of the coronary, brachial, femoral and pulmonary artery are 0.0015, 0.0017, 0.0033 and 0.0135 m respectively. The corresponding Womersley number are 9, 13.6, 6.4 and 21.8. Whale *et al.*[42] measured the permeability of an ostensibly healthy human aortic wall for the cylindrical geometry to be $1.7 \pm 0.2 \times 10^{-18}$ m^2 and we have used this value. Following Tzirtzilakis,[38] the electrical conductivity of blood 0.7 S m^{-1} as measured by Gabriel *et al.*[12] has been used. In the present study, the number of harmonics used in the Fourier series expansion of the pressure gradient waveforms for human coronary, brachial, femoral and pulmonary artery are 50, 60, 50 and 50 respectively. The details of the Fourier co-efficients involved in the Fourier series approximations (McDonald's model) and the corresponding root mean square errors for the four arteries considered here are presented in our earlier articles.[13,14] The SMF strength is varied from high (1T–3T), very high (3T–7T) and then ultra high intensity (> 7T). The values of Hartman number are computed in all the four arteries for various strengths of the applied magnetic field ranging from 0T to 20T and are provided in Table 1.

Based on the analytical expression for the velocity of blood in the artery provided in "Mathematical Formulation and Solution", the mean center-line velocity and the mean WSS over a cardiac cycle are calculated using the time averaged magnitude of velocity and WSS respectively and are tabulated in Tables 2, 3, 4, and 5 for various SMF strengths. Further, medically significant HWPs such as TAWSS, OSI

TABLE 3. HWPs of brachial artery for various magnetic field strength.

Brachial artery-HWPs	0*T*	1.5*T*	3*T*	5*T*	8*T*	10*T*	20*T*
Mean velocity (m/s)	0.3068	0.3067	0.3063	0.3056	0.3037	0.302	0.2884
% Change		− 0.04	− 0.14	− 0.40	− 1.00	− 1.56	− 5.98
Mean WSS (Pa)	− 1.0907	− 1.0905	− 1.0897	− 1.0878	− 1.0834	− 1.0794	− 1.0471
% Change	–	0.02	0.10	0.26	0.70	1.04	4.00
OSI	0	0	0	0	0	0	0
RRT (N/m^2)	0.9172	0.9174	0.9181	0.9196	0.9234	0.9268	0.9554
% Change	–	0.0237	0.0949	0.2636	0.6738	1.0515	4.1627
Peak velocity (m/s)	0.4086	0.4085	0.4081	0.4073	0.4053	0.4035	0.3892
% Change	–	− 0.0245	− 0.1224	− 0.3182	− 0.8076	− 1.2482	− 4.7479
Minimum velocity (m/s)	0.2651	2.650	0.2647	0.2639	0.2621	0.2604	0.2472
% Change	–	− 0.0377	− 0.1509	− 0.4527	− 1.1316	− 1.7729	− 6.7522
Peak WSS (Pa)	− 0.8804	− 0.8801	− 0.8792	− 0.8772	− 0.8724	− 0.8680	− 0.8327
% Change	–	− 0.0341	− 0.1363	− 0.3635	− 0.9087	− 1.4085	− 5.4180
Minimum WSS (Pa)	− 1.867	− 1.8660	− 1.8650	− 1.8630	− 1.8590	− 1.8540	− 1.8190
% Change	–	− 0.0536	− 0.1071	− 0.2142	− 0.4285	− 0.6963	− 2.5710

TABLE 4. HWPs of femoral artery for various magnetic field strength.

Femoral artery-HWPs	0*T*	1.5*T*	3*T*	5*T*	8*T*	10*T*	20*T*
Mean velocity (m/s)	0.0525	0.0524	0.0523	0.052	0.0514	0.0508	0.0462
% Change		− 0.08	− 0.31	− 0.85	− 2.14	− 3.30	− 12.07
Mean WSS (Pa)	− 0.1272	− 0.1272	− 0.1270	− 0.1265	− 0.1254	− 0.1244	− 0.1169
% Change		0.05	0.20	0.56	1.43	2.20	8.1
OSI	0.1925	0.1927	0.1930	0.1938	0.1958	0.1975	0.2114
% Change		0.06	0.24	0.66	1.67	2.6	9.8
RRT (N I m^2)	7.8622	7.8662	7.8782	7.9067	7.9758	7.9412	8.0421
% Change		0.05	0.20	0.57	1.45	1.01	2.23
Peak velocity (m/s)	0.1103	0.1102	0.1101	0.1099	0.1093	0.1089	0.1052
% Change	–	− 0.0907	− 0.1813	− 0.3626	− 0.9066	− 1.2693	− 4.6238
Minimum velocity(m/s)	− 0.0124	− 0.01246	− 0.01257	− 0.01283	− 0.01346	− 0.01402	− 0.0182
% Change		0.3221	1.2077	3.3011	8.3736	12.8824	46.5378
Peak WSS (Pa)	0.25	0.2501	0.2503	0.2509	0.2522	0.2533	0.2624
% Change		0.04	0.12	0.36	0.88	1.32	4.96
Minimum WSS (Pa)	− 0.674	− 0.6739	− 0.6738	− 0.6733	− 0.6723	− 0.6714	− 0.6645
% Change		− 0.0148	− 0.0297	− 0.1039	− 0.2522	− 0.3858	− 1.4095

TABLE 5. HWPs of pulmonary artery for various magnetic field strength.

Pulmonary artery-HWPs	0*T*	1.5*T*	3*T*	5*T*	8*T*	10*T*	20*T*
Mean velocity (m/s)	0.1347	0.1330	0.1281	0.1178	0.0981	0.0848	0.0382
% Change		− 1.27	− 4.89	− 12.56	− 27.14	− 37.04	− 71.61
Mean WSS (Pa)	− 0.0798	− 0.0791	− 0.0772	− 0.0731	− 0.0651	− 0.0596	− 0.0385
% Change		0.85	3.27	8.43	18.40	25.34	51.79
OSI	0.4354	0.4360	0.4375	0.4408	0.4472	0.4517	0.4687
% Change		0.13	0.48	1.24	2.71	3.73	7.65
RRT (N/m^2)	12.5331	12.6399	12.9567	13.6873	15.3601	16.7785	25.9740
% Change		0.85	3.38	9.21	22.55	32.74	100.47
Peak velocity (m/s)	0.3374	0.3357	0.3309	0.3206	0.3012	0.2880	0.2429
% Change	–	− 0.5039	− 1.9265	− 4.9793	− 10.7291	− 14.6414	− 28.008
Minimum velocity(m/s)	− 0.00153	− 0.0033	− 0.008196	− 0.01865	− 0.03859	− 0.0522	− 0.1011
% Change	–	112.240	433.594	1114.193	2412.370	3298.438	6482.031
Peak WSS (Pa)	1.671	1.671	1.674	1.678	1.686	0.693	1.718
% Change	–	0	0.1795	0.4189	0.8977	1.3166	2.8127
Minimum WSS (Pa)	− 2.436	− 2.435	− 2.434	− 2.429	− 2.422	− 2.416	− 2.396
% Change	–	− 0.0411	− 0.0821	− 0.2874	− 0.5747	− 0.8210	− 1.6420

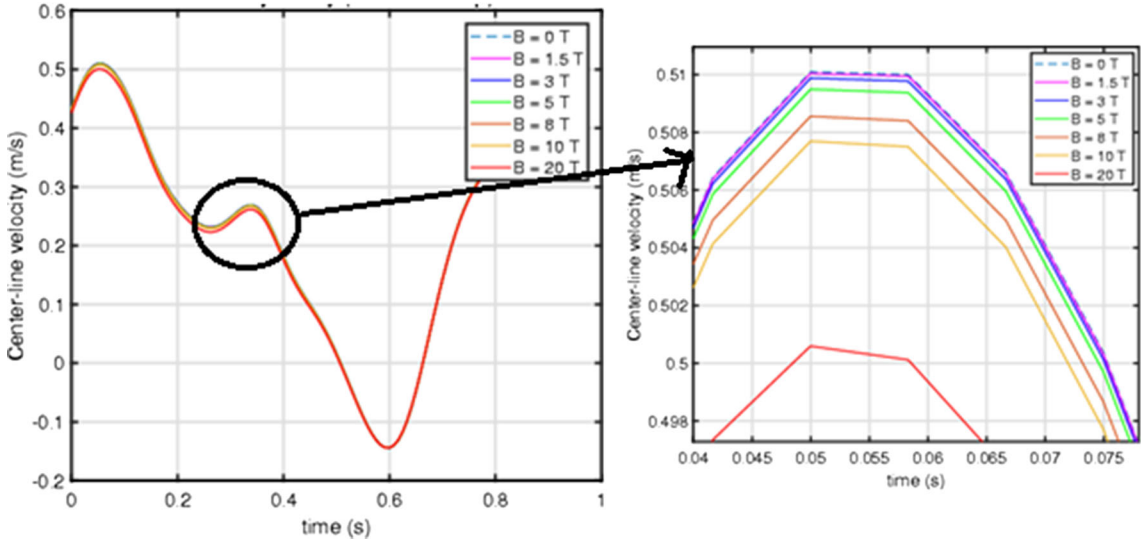

FIGURE 2. Mean center line velocity of coronary artery.

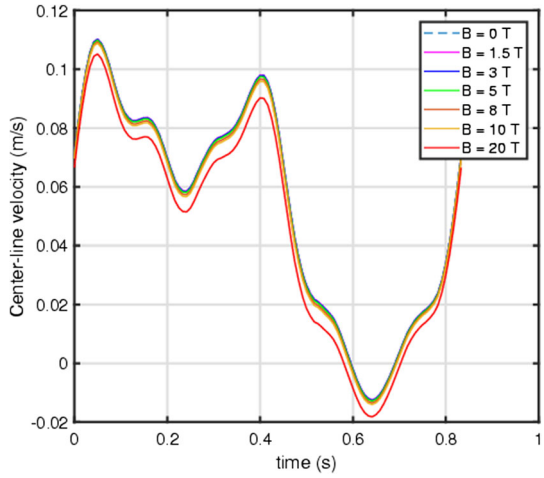

FIGRUE 3. Mean center-line velocity of femoral artery.

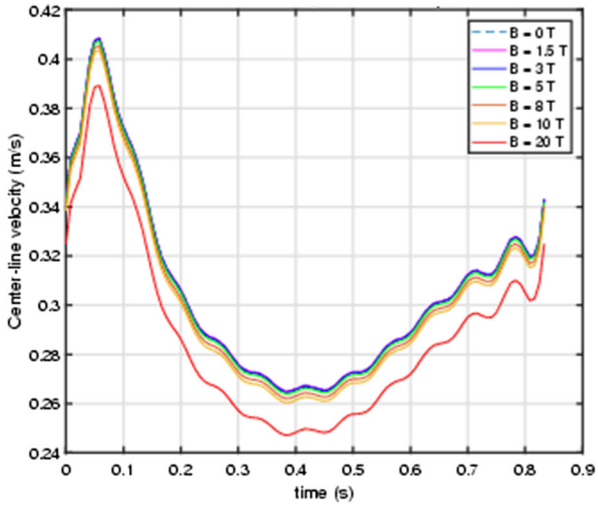

FIGURE 4. Mean center-line velocity of brachial artery.

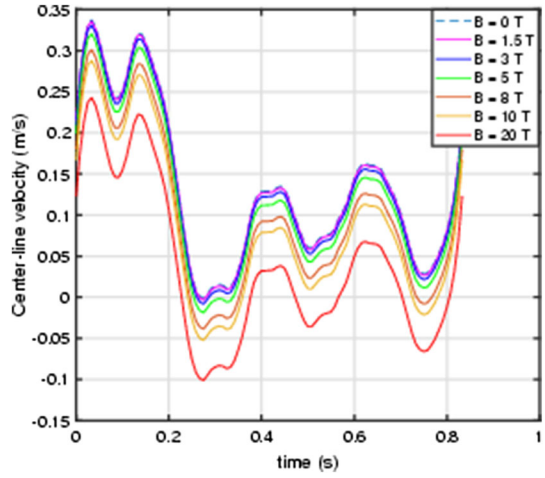

FIGURE 5. Mean center-line velocity of pulmonary artery.

and RRT are also computed numerically and are tabulated in Tables 2, 3, 4, and 5. Further, to quantify the effect of magnetic field on HWPs, the percentage of change for the mean velocity, TAWSS, OSI and RRT are also presented in Tables 2, 3, 4, and 5. The dimensional velocity and WSS waveforms for all the four arteries are plotted in Figs. 2, 3, 4, 5, 6, 7, 8, and 9 for various SMF strengths.

Velocity Profile

Depending on the dynamic needs of the organs in various locations of CVS, blood flow is initiated through arteries. Sufficient blood flow is crucial for adequate supply of oxygen and nutrients to all the tissues, which is directly related to longevity and quality of life that includes cardiovascular health.

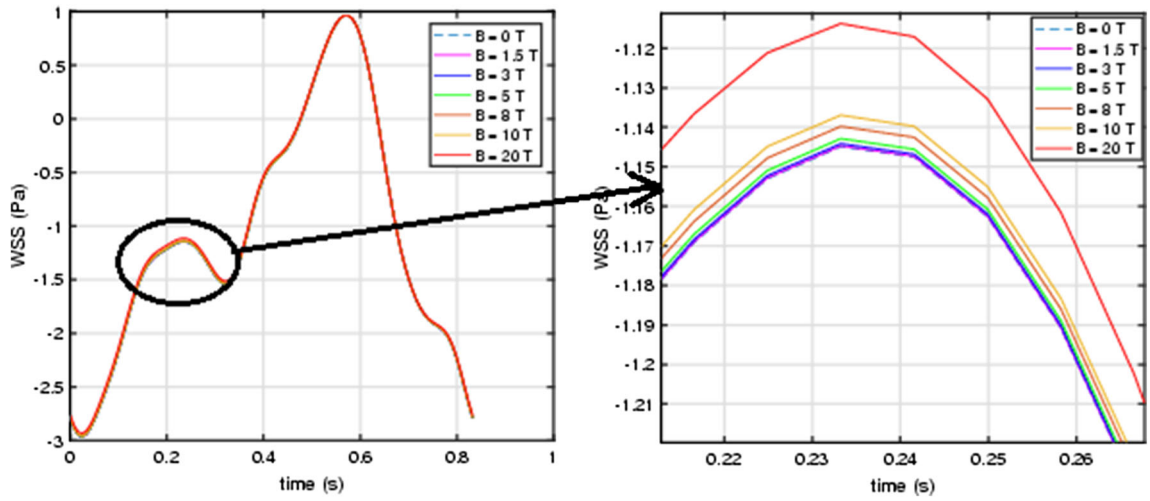

FIGURE 6. WSS of coronary artery for various magnetic field strength.

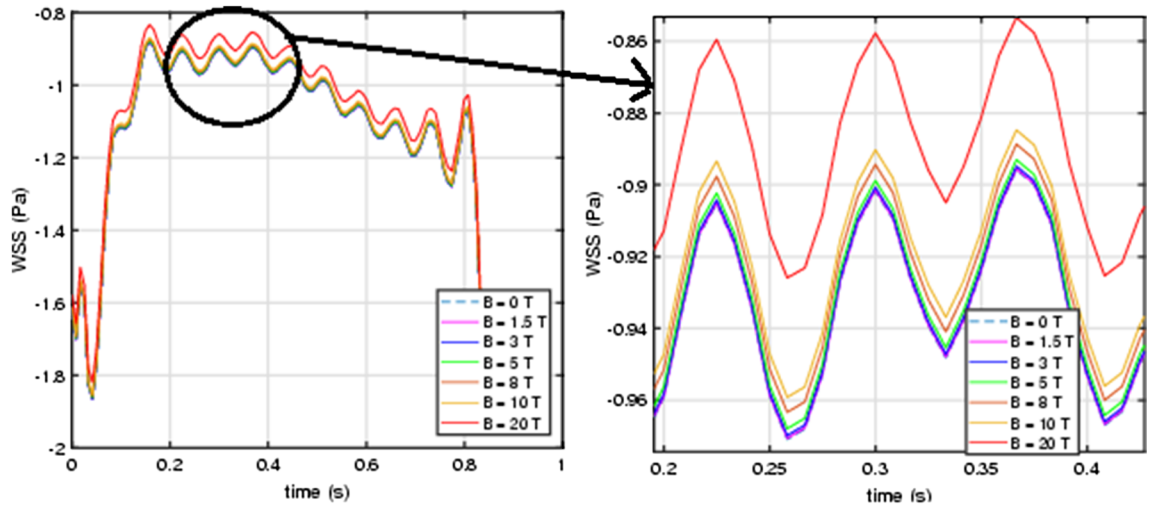

FIGURE 7. WSS of brachial artery for various magnetic field strength.

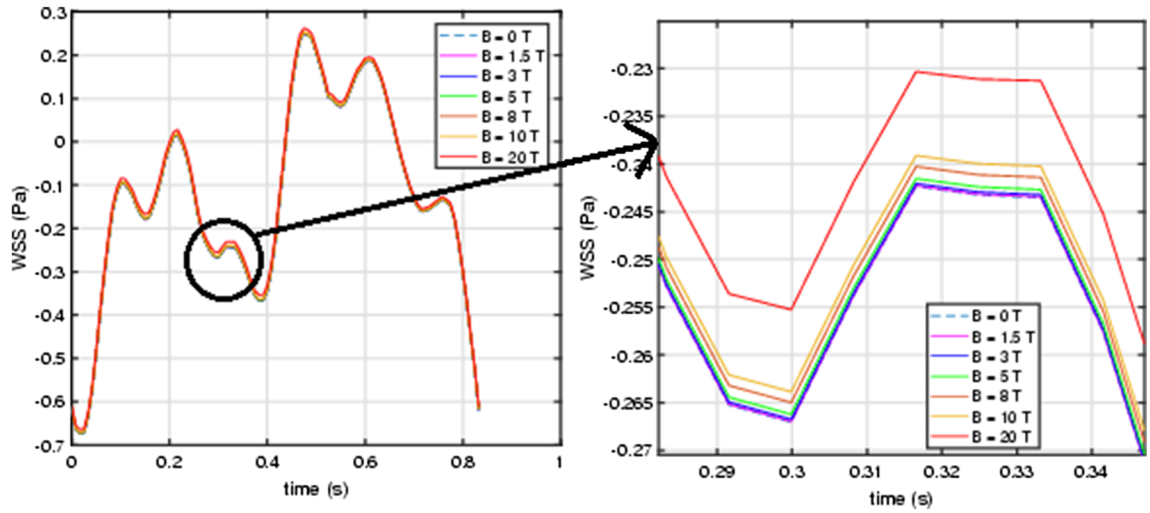

FIGURE 8. WSS of femoral artery for various magnetic field strength.

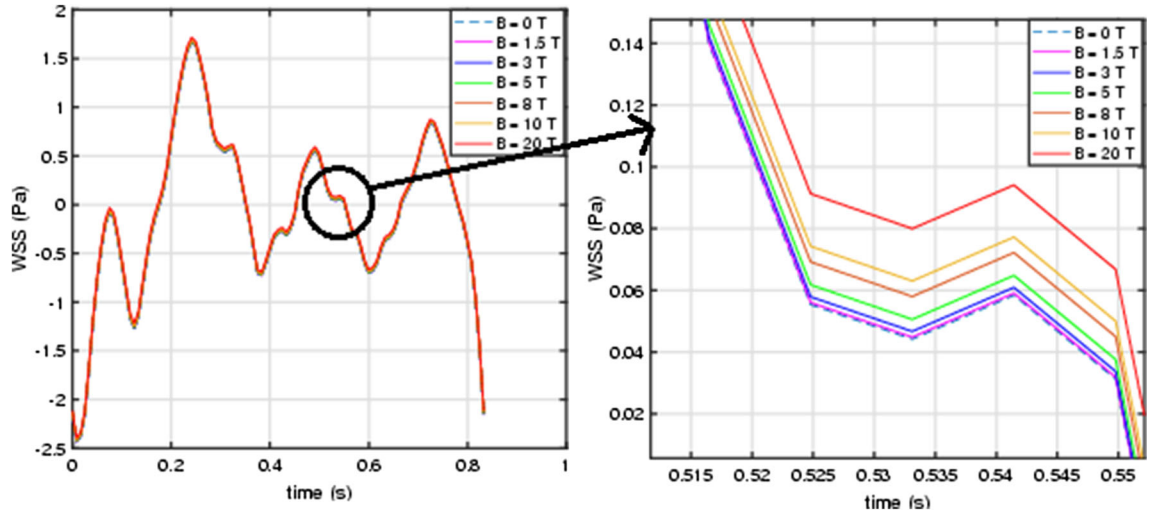

FIGURE 9. WSS of pulmonary artery for various magnetic field strength.

Occlusion in the blood vessels in various locations will cause disturbances in the normal velocity of blood. Majority of CVDs and disorders are due to the hemodynamic dysfunction. Indeed, the velocity of blood in the lumen plays a vital role by modulating the vascular response by kindling the endothelium to release nitric oxide (NO). Hence, an estimation of blood velocity in the presence of SMF is crucial for understanding the clinical consequences as explained below.

The mean center line velocity of the coronary, brachial, femoral and pulmonary arteries estimated for $M = 0$ (non-magnetic case) in the present analysis are 0.2073, 0.3068, 0.0525 and 0.1347 m/s respectively. The corresponding values reported in the medical literature for the non-magnetic case by Ofili *et al.*,[30] Sinoway *et al.*,[34] Shoemaker *et.al.* [32] and Ivor *et al.*[11] are 0.40 ± 0.19, 0.295, 0.089 ± 0.03 and 0.13 m/s respectively. It is interesting to note here that the obtained results in Figs. 2, 3, 4, 5; Tables 2, 3, 4, 5 are in good agreement with the reported results in the medical literature and also with our earlier work[14] for the non magnetic study of pulsatile blood flow in large arteries.

The percentage of reduction in the mean center line velocity of blood in the coronary artery is only 0.02% at 1.5 T whereas it shoots up to 0.7 and 2.74% at 10 and 20 T respectively (refer Table 2). Since coronary artery supplies blood to the surrounding muscles of the heart, the clinical significance of 2.74% reduction in blood velocity may have to be carefully considered.

At the same time, in brachial and femoral arteries which are located at the lower extremity (arms) and upper extremity (legs), the percentage of reduction in mean center line velocity of blood are 0.04, 0.08% at 1.5 T, 1.56, 3.3% at 10 T and 5.98, 12.07% at 20 T respectively. The percentage of reduction in blood velocity estimated by us is less in brachial than in femoral segment as the SMF strength increases. When comparing these arteries with that of coronary artery, the percentage of reduction in coronary segment is even more less. Further, it is to be noted here that the estimated percentage of reduction in the velocity of blood in the pulmonary artery are 1.27, 37.04 and 71.61% at 1.5 , 10 and 20 T respectively. Thus, it is observed that as the radius of the artery increases, the effect of SMF on blood velocity also increases. This is due to the fact that the Hartmann number depends on the radius of the artery. Indeed, as the radius of the artery increases the corresponding Hartmann number also increases and the required data are provided in Table 1. The possibility of less oxygen transport from lung to heart due to high reduction in blood velocity at high intensity SMF is to be critically examined. Incidentally, Kangarlu *et al.*[20] reported that under ultra high SMF (7T) human beings undergo the risk of ventricular fibrillation and arhythmogenic cardiac simulation and that this risk has to be medically assessed.

However, the peak centre line velocity is reduced by 0.02, 0.03, 0.09 and 0.5% for the coronary, brachial, femoral and pulmonary artery respectively at 1.5T, whereas Abi Abdallah *et al.*[1] estimated this to be around 0.09%. In the ultra high SMF (8T), the above reductions in peak centre line velocity shoot up to 0.29, 0.81, 0.91 and 10.73% respectively in the above arteries, whereas Abi Abdallah *et al.*[1] predicted this to be slightly higher than 2.5%. At 20T, the reduction in peak centre-line velocity is found to be 1.86, 4.74, 4.62 and 28% respectively in the coronary, brachial, femoral and pulmonary artery. The corresponding Hartmann numbers are 0.39, 0.58, 0.85 and 3.49

respectively. Incidentally, Abi Abdallah *et al.*[1] predicted a reduction of 34.5% at $40T$ ($M = 4.47$) and Keltner *et al.*[21] noted a reduction of 30% for $M = 4$. On the other hand, we have noticed a reduction of 2.74, 5.98, 12.07 and 71.61% in the mean centre line velocity of the coronary, brachial, femoral and pulmonary artery respectively at $20T$ with corresponding M given in Table 1. We believe that our estimations are more accurate than Abi Abdullah *et al.*[1] since they have considered a simplified mathematical modeling by assuming the pressure gradient to be equivalent to the one that would produce Poiseuille flow with a mean velocity of 0.4 m/s which is not true in all the arteries.

Hemodynamic Wall Parameters

Root cause of CVD remains to be perplexing and enigmatic. However, hemodynamics is identified as a key factor in promoting degenerative effects and pathologies affecting several vascular diseases. The details of blood velocity alone does not provide the complete response of the endothelial layer due to the magnetic field exposure. Flow driven mechanisms that provide additional information are (i) effects of SMF on endothelial function based on WSS and (ii) alterations in the residence time of the atherogenic particles near the wall. In order to understand the consequences due to the reduction of blood velocity and the possible pathological changes of the artery, HWPs such as TAWSS, OSI and RRT are to be found and analysed collectively. In this Section, the abovesaid parameters are analyzed for the four arteries considered.

It is observed from Tables 2, 3, 4, and 5 that the effect of magnetic field on the magnitude of WSS, a medically relevant HWPs, is to decrease it. Physically, if a uniform magnetic field is applied in the transverse direction on the blood flow, the velocity in the core region is reduced since the Lorentz force is proportional to the velocity. As a result, the parabolic velocity profile becomes flattened and also the magnitude of the shear rate $\partial u/\partial r$ decreases as the magnetic field strength increases. In short, the magnetic field reduces the magnitude of WSS. It cannot be over emphasized here that even a slight change in the direction of velocity vector near the wall will result in enormous change in the shear rate $\partial u/\partial r$ and hence the WSS.

It is to be noted here that the magnitude of mean WSS for the coronary, brachial, femoral and pulmonary artery reported in the medical literature for non-magnetic case (i.e. when $M = 0$) by He and Ku[18] Verbeke *et al.*,[40] Kornet *et al.*[24] and Tang *et al.*[35] are 1.6, 1.9 ± 0.12, 0.35 ± 0.18 and 0.13 ± 0.28 Pa respectively. Our estimated results in the present analysis for the magnitude of mean WSS in the abovesaid arteries are 1.1055, 1.0907, 0.1272 and 0.0798 Pa respectively. Further, OSI value for the brachial, femoral, coronary and pulmonary artery reported in the medical literature for non-magnetic case (i.e. when $M = 0$) by Thosar *et al.*,[37] He and Ku[18] and Masaki Terada *et al.*[36] are 0.09 ± 0.09, 0.27 ± 0.1, 0.08 and 0.214 ± 0.026 whereas the corresponding OSI estimated in the present analysis are 0.1925, 0, 0.0864 and 0.4354 respectively. Hence, the obtained results for the case of $M = 0$ are in reasonably good agreement with the reported results in the medical literature and also in exact agreement with our earlier work.[14] This indicates that our mathematical modeling is reliable.

It is observed from the graphs of WSS waveform (Figs. 6, 7, 8, and 9) that in all the four arteries considered here, irrespective of the site of the arteries, whether it is closer to the heart or far away from the heart, the absolute value of WSS decreases as the magnetic field strength increases. Malek *et al.*[26] has reported that the WSS range for a normal artery is 1 to 7 Pa and for an atherosclerotic prone artery is $\pm$ 0.4 Pa. Based on this, it is inferred that the coronary and brachial segments of the respective subjects are in the normal shear range which are free from the formation of atherosclerosis whereas the femoral and pulmonary segments of the respective subjects are in low shear region which are prone to the formation of the atherosclerosis. It is worth to notice here that even when SMF strength is increased up to $20T$, in none of the arteries the region gets shifted from the abovesaid normal range to the atherosclerotic prone range. As the radius of the artery increases, the percentage of reduction in the magnitude of WSS also increases (refer Tables 2, 3). We find that the value of WSS are different in different arteries and hence the general assumption that physiological WSS is 1.5 Pa throughout the human vascular tree is untenable as indicated by Cheng *et al.*[5]

The magnitude of WSS at a particular location alone cannot help us to understand the abnormalities in the flow dynamics and hence it is essential to study the directional changes of WSS vector as indicated by OSI (refer "Oscillatory Shear Index (OSI)") to get a better picture of the same. Indeed, He and Ku[18] have mentioned that OSI is known to correlate strongly with intimal thickening in the arteries.

Now, we would like to compare the OSI and RRT values of the coronary and brachial arteries whose WSS values are found to be in the normal range. OSI value of the coronary and brachial artery indicates that though in both the arteries WSS range is normal, WSS vector need not be unidirectional. It is evident from Fig. 7 that the WSS vector of brachial artery is negative throughout a cardiac cycle whatever be the mag-

netic field strength and hence its OSI value is zero. Further, it is apparent from Fig. 6 that in a cardiac cycle, in the presence of magnetic field, WSS vector of the coronary artery changes its sign from negative to positive and then to negative only once during 0.4 to 0.7 s, for all possible value of SMF strength and hence, the value of OSI is not zero. As the magnetic field strength increases, the fluctuation in the direction of WSS vector also increases in the coronary artery (refer Table 2).

The value of RRT represents the prolongation of blood particles near the wall. RRT value also varies in both the artery as the SMF strength is varied. This variation is notable in the coronary artery in comparison to the brachial artery (refer Tables 2, 3).

Now, let us compare the OSI and RRT values of the femoral and pulmonary arteries whose WSS values are found to be in the low shear range prone to the formation of atherosclerosis. OSI values of these arteries indicate that though in both the arteries WSS is in low shear range, the direction of WSS vectors need not oscillate heavily from time to time in a cardiac cycle. In the femoral artery, OSI value varies from 0.1925 to 0.2114 whereas in the pulmonary artery it varies between 0.4354 and 0.4687 as SMF strength is varied from 0 to 20T. It is evident from Figs. 8, 9 that WSS vector is changing sign from negative to positive and then to negative twice in a cardiac cycle during 0.175 to 0.3 s and 0.4 to 0.7 s in the femoral artery and thrice in a cardiac cycle during 0.2 to 0.3 s, 0.4 to 0.6 s and 0.6 to 0.8 s in the pulmonary artery. This is the reason for the difference in the OSI values of these two arteries. Further, the OSI value in the femoral artery is moderate (being closer to 0.2) whereas in the pulmonary artery it is very severe (being closer to 0.5). At 20T (ultra high intensity) OSI shoots up by 9.8% in the femoral artery which is numerically higher than in the pulmonary artery in which it is 7.65%. But, the magnetic field effect is more in the pulmonary as the OSI value is closer to 0.5 than the femoral whose OSI value is closer to 0.2. Hence, based on the combined effect of TAWSS and OSI value, the subject of femoral artery may be classified as moderately affected and the subject of pulmonary artery as severely affected owing to high/ultra high intensity SMF. This conclusion is further supported by the RRT values. The suspended atherogenic particles in the blood spends more time near the pulmonary arterial wall than that of the femoral and this residence time is more as we increase the SMF strength from high to ultra high intensity (refer Tables 4, 5). Hence, our results strongly point out that at low shear region, OSI need not be high, even in the presence of magnetic field. This result is in good agreement with our earlier observations.[13–15]

Finally, it is also inferred from Figs. 2, 3, 4, 5, 6, 7, 8, and 9 that whenever there is a peak in velocity, WSS is minimum and vice versa in all the arteries for various SMF strengths. Further, comparing the values of RRT in all the four arteries for various SMF strengths, it is found that larger the value of Womersley number, larger the RRT and hence higher the probability for vascular diseases.

In summary, the effect of magnetic field on HWPs in all the four arteries considered here increases as the magnetic field strength increases from high to very high and then to ultra high. In particular, the velocity decreases and the absolute value of WSS decreases as the SMF strength increases from high to ultra high intensity magnetic field irrespective of the site of the arteries, whether it is closer to the heart or far away from the heart. Flow retardation and the flattening of the instantaneous parabolic profile are significant in the pulmonary artery because it is in this artery the Hartmann number is the largest. Up to 3T no significant change is observed in the hemodynamic parameters of all the four arteries except for the pulmonary artery in which changes in the velocity and RRT are discernible. Beyond 8T all the parameters in all the four arteries are affected, but the changes are very significant only in the pulmonary artery. We strongly believe that there is a possibility for adverse effects in the pulmonary hemodynamics, in particular in HWPs, while exposing the human beings to ultra high intensity SMF at least at the time of exposure.

Davies[8] has documented the severity of CVDs based on the range of WSS. However, we find that no such documentation is available on the aetiology, pathogenesis and severity of CVDs based on OSI and RRT despite the fact that these metrics have been developed long ago. In this sense, the present work can be considered as an elementary work comparing the effect of SMF on the hemodynamics in all the three circulations. However, the results reported here are to be validated by similar studies on a large number of subjects and the analyses and interpretations of the clinical consequences of the results thereof are to be documented carefully.

It is to be noted here that we have employed the pressure gradient waveforms of different subjects in different arteries. Hence, the values of all the parameters are not only artery specific but also subject specific. Thus, the effect of SMF on these parameters may vary from person to person, since even the radius of the same artery may be different in two different subjects and the Hartmann number depends on the radius of the artery. This also indicates that one cannot conclude anything about the effect of magnetic field on blood flow in human beings based on experimental studies on animals. It may be recalled that the values of all these

parameters significantly vary species to species as explained by Cheng *et al.*[5]

Since the pressure gradient waveforms employed in this analysis are subject specific, this type of analysis should be repeated on more number of subjects before benchmarking the results for medical purposes. We have not taken into consideration the effect of the pulse frequency $f = \omega/2\pi$ (which is fixed as 72 beats per minute) and hence similar studies are recommended by using the pressure gradient waveform of subjects with tachycardia.

All the above analyses where repeated during our computation using the Saffman slip condition, the analytical solutions for which are reported in Appendix 4. It is inferred that there is absolutely no difference in the results obtained both qualitatively and quantitatively for various SMF strengths in all the four arteries. This may be due to the fact that Saffman slip condition is applicable for a densely packed porous wall of infinite thickness whereas the arterial wall is of finite thickness and all the layers of the arterial wall except the endothelial layer is sparsely packed. Further, the existing interfacial conditions available in the literature of flow through tubes with porous walls may not be suitable for the hemodynamic studies.[41]

CONCLUSIONS

To the best of our knowledge, this is the first elaborate qualitative and quantitative theoretical study comparing the effect of high/ultra high SMF on the velocity of blood and HWPs believed to be responsible for the pathogenesis of atherosclerosis in all the three circulations. This study has been carried out with an assumption that the applied magnetic field is transverse or perpendicular to the flow direction. Subject to this assumption the major conclusions of our investigation are as follows:

1. There are no significant adverse effects in any of the arteries considered here up to 3 T except for a discernible change in the velocity and RRT of the pulmonary artery. However, beyond $8T$ very significant effect on HWPs are noticed in the pulmonary artery and it is inferred that in such cases proper clinical assessment and monitoring may be required while exposing human subjects to such high intensity SMF.
2. The common hypothesis that low WSS and high OSI co-locate is not tenable even in the presence of magnetic field though individually both may contribute to CVDs.
3. It is inferred that one cannot conclude anything about the effect of magnetic field on blood flow in human beings based on experimental studies on animals and this may be one of the reasons for many existing contradicting reports in the literature. It is high time that this fact is recognized and the experimental or empirical results using animal specifies are discriminated from the analytical results reported on human beings.

We strongly feel that more number of active and intensive patient specific research similar to the one presented here may throw some light towards documenting the clinical consequences of high intensity SMF on hemodynamics and this study can only be considered as a preliminary and primitive one in these lines.

Further, in addition to the above results we also found that the results are not significantly different when the Saffman slip condition is used instead of no slip condition and hence we recommend that an appropriate slip condition at the lumen-wall interface is to be developed soon.

It is strongly recommended that future research must focus on more realistic problem of analyzing the effects of orientation of SMF to the flow direction by considering a curved artery of non-uniform cross section, perhaps with wall distensibility.

APPENDIX 1

Let $\overline{B}$ be in the direction transverse to the flow direction (x-axis). Then, the velocity and magnetic field are $\overline{q} = [0, 0, u]$ and $\overline{B} = [B_0, 0, 0]$ in the Cartesian coordinate system. Then

$$\bar{j} = \sigma[\overline{q} \times \overline{B}] = \sigma \begin{vmatrix} \hat{e}_x & \hat{e}_y & \hat{e}_z \\ 0 & 0 & u \\ B_0 & 0 & 0 \end{vmatrix} = \sigma[0, uB_0, 0] \quad (14)$$

Hence, the Lorentz force

$$\bar{j} \times \overline{B} = \sigma \begin{vmatrix} \hat{e}_x & \hat{e}_y & \hat{e}_z \\ 0 & uB_0 & 0 \\ B_0 & 0 & 0 \end{vmatrix} = \sigma[0, 0, -uB_0^2] \quad (15)$$

Similarly, we can get $\bar{j} \times \overline{B} = \sigma[0, 0, -uB_0^2]$ even when the magnetic field is applied in the direction perpendicular to the flow direction (y-axis).

APPENDIX 2

It may be recalled that the magnetic Reynolds number R_m is the ratio of the induced magnetic field to the applied magnetic field. It is given by $R_m = \frac{UR}{\eta}$ where $\eta = \frac{1}{\mu_e \sigma}$ denotes the magnetic diffusivity. Here, $\mu_r = \frac{\mu_e}{\mu_0}$ denotes the relative permeability of the blood. $\mu_0 = 1.26 \times 10^{-6}$ H/m and $\sigma = 0.7$ S/m denote the permeability of free space and the electrical conductivity of the blood respectively. Now,

$$R_m = \mu_e \sigma UR = \mu_r \mu_0 \sigma UR = (1 + \chi)\mu_0 \sigma UR \qquad (16)$$

where χ denotes the magnetic susceptibility of the blood and U denotes the characteristic velocity of the blood in the respective artery. Further, the magnetic susceptibility of oxygenated and deoxygenated blood are $\chi = -6.6 \times 10^{-7}$ and $\chi = 3.5 \times 10^{-6}$ respectively. Thus, R_m is estimated as follows.

Artery	Radius (R)	Velocity (U)	R_m
Coronary artery	0.0015	0.2073	2.7×10^{-10}
Brachial artery	0.0023	0.3068	6.2×10^{-10}
Femoral artery	0.0033	0.0525	1.5×10^{-10}
Pulmonary artery	0.0135	0.1347	1.6×10^{-9}

APPENDIX 3

The method of arriving at the solutions given in Eq. (10) from the Eqs. (8) and (9) with the prescribed boundary conditions is given below: By taking $\overline{V} = \overline{u} - \frac{p_0 R}{\mu \omega M^2}$ in Eq. (8) reduces it to the homogeneous modified Bessel equation

$$\frac{\partial^2 \overline{V}}{\partial r^2} + \frac{1}{r}\frac{\partial \overline{V}}{\partial r} - M^2 \overline{V} = 0 \qquad (17)$$

Further, putting $Z = rM$ in the above Eq. (17), we get

$$Z^2 \frac{\partial^2 \overline{V}}{\partial Z^2} + Z \frac{\partial \overline{V}}{\partial Z} - Z^2 \overline{V} = 0 \qquad (18)$$

The general solution of the above modified Bessel equation of order zero is given by

$$\overline{V}(Z) = C_1 I_0(Z) + C_2 K_0(Z) \qquad (19)$$

C_2 becomes zero since $\overline{u}$ is finite, when $r = 0$ and $C_1 = -\frac{p_0 R}{\mu \omega M^2 I_0(M)}$ since $\overline{u} = \overline{u}_B = 0$, when $r = 1$. Thus, the steady part of velocity $u(r, t)$ is $\overline{u}(r) = C_1 I_0(Mr) + \frac{p_0 R}{\mu \omega M^2}$.

Similarly, substituting $\tilde{V}_n = \tilde{u}_n - \frac{p_n R}{\mu \omega G_n}$, Eq. (9) reduces it to the homogeneous modified Bessel equation

$$\frac{\partial^2 \tilde{V}_n}{\partial r^2} + \frac{1}{r}\frac{\partial \tilde{V}_n}{\partial r} - \left(M^2 + in\alpha^2\right)\tilde{V}_n = 0 \qquad (20)$$

Further, putting $Z_n = r\sqrt{M^2 + in\alpha^2}$ in the above Eq. (17), we get

$$Z^2 \frac{\partial^2 \tilde{V}_n}{\partial Z^2} + Z \frac{\partial \tilde{V}_n}{\partial Z} - Z^2 \tilde{V}_n = 0 \qquad (21)$$

The general solution of the above modified Bessel equation of order zero is given by

$$\tilde{V}_n(Z_n) = C_3 I_0(Z_n) + C_4 K_0(Z_n) \qquad (22)$$

C_4 become zero since $\tilde{u}_n$ is finite, when $r = 0$ and $C_3 = \frac{-p_n R}{\mu \omega (M^2 + in\alpha^2) I_0\left(\sqrt{M^2 + in\alpha^2}\right)}$ since $\tilde{u}_n = \tilde{u}_{B_n} = 0$, when $r = 1$. Thus, the nth harmonic of unsteady part of velocity $u_n(r, t)$ is $\tilde{u}_n(r) = C_3 I_0\left(\sqrt{M^2 + in\alpha^2} r\right) + \frac{p_n R}{\mu \omega (M^2 + in\alpha^2)}$.

APPENDIX 4

The non-dimensional equations for the steady part of the velocity $\overline{u}$ and the nth harmonic of the oscillatory part of the velocity $\tilde{u}_n$ are given in the Eqs. (8) and (9) respectively. Their corresponding Saffman slip conditions are given by

$$\overline{u} \text{ is finite, when } r = 0;\ \overline{u}_B = -\left(\frac{\sqrt{k}}{R\overline{\alpha}}\right)\frac{\partial \overline{u}}{\partial r}, \text{ when } r = 1$$

$$\tilde{u}_n \text{ is finite, when } r = 0;\ \tilde{u}_{B_n} = -\left(\frac{\sqrt{k}}{R\overline{\alpha}}\right)\frac{\partial \tilde{u}_n}{\partial r}, \text{ when } r = 1$$

Here, k and $\overline{\alpha} = 0.01$ denote the permeability of the arterial wall and the Beavers Joseph slip coefficient[13] respectively. Solving the above equations using the details provided in Appendix 3, we get the values for the constants C_1, C_2, C_3 and C_4 in the Eqs. (19) and (22) in the Appendix 3 as C_2 becomes zero since $\overline{u}_B$ is finite, when $r = 0$ and $C_1 = \left[\left(-\frac{p_0 R}{\mu \omega M^2}\right)(I_0(M) + \frac{\sqrt{k} M}{R\overline{\alpha}} I_1(M))\right]^{-1}$ since $\overline{u}_B = -\left(\frac{\sqrt{k}}{R\overline{\alpha}}\right)\frac{\partial \overline{u}}{\partial r}$, when $r = 1$. C_4 becomes zero since $\tilde{u}_{B_n}$ is finite, when $r = 0$ and since $\tilde{u}_{B_n} = -\left(\frac{\sqrt{k}}{R\overline{\alpha}}\right)\frac{\partial \tilde{u}_n}{\partial r}$, when $r = 1$, we have $C_3 = \left[\left(\frac{-p_n R}{\mu \omega (M^2 + in\alpha^2)}\right)\left(I_0\left(\sqrt{M^2 + in\alpha^2}\right) + \frac{\sqrt{k(M^2 + in\alpha^2)}}{R\overline{\alpha}} I_1\left(\sqrt{M^2 + in\alpha^2}\right)\right)\right]^{-1}$. Hence, the velocity of blood in the lumen of the artery and the slip velocity at the wall when the Saffman slip is employed at the lumen wall interface are given by

$$u(r,t) = \frac{p_0 R}{\mu\omega M^2}\left[1 - \frac{I_0(Mr)}{I_0(M) + \left(\sqrt{k}M/R\overline{\alpha}\right)I_1(M)}\right] + Re\sum_{n=1}^{m}\left[\frac{p_n R}{\mu\omega(M^2 + in\alpha^2)}\left[1 - \frac{I_o\left(\sqrt{M^2 + in\alpha^2}r\right)}{I_o\left(\sqrt{M^2 + in\alpha^2}\right) + \left(\sqrt{k(M^2 + in\alpha^2)}/R\overline{\alpha}\right)I_1\left(\sqrt{M^2 + in\alpha^2}\right)}\right]e^{i(n\omega t - \gamma_n)}\right] \tag{23}$$

$$u_B(t) = \frac{-p_0 R}{\mu\omega M^2}\left[\frac{MI_1(M)}{I_0(M) + \left(\sqrt{k}M/R\overline{\alpha}\right)I_1(M)}\right] + \quad Re\sum_{n=1}^{m}\left[\frac{-p_n R}{\mu\omega(M^2 + in\alpha^2)}\left[\frac{\sqrt{M^2 + in\alpha^2}I_1\left(\sqrt{M^2 + in\alpha^2}\right)}{I_o\left(\sqrt{M^2 + in\alpha^2}\right) + \left(\sqrt{k(M^2 + in\alpha^2)}/R\overline{\alpha}\right)I_1\left(\sqrt{M^2 + in\alpha^2}\right)}\right]e^{i(n\omega t - \gamma_n)}\right] \tag{24}$$

where I_0 and I_1 are the modified Bessel function of order zero and one, respectively.

CONFLICT OF INTEREST

Gayathri K. and Shailendhra K. declare that they have no conflict of interest.

ETHICAL APPROVAL

This article does not contain any studies with human participants or animals performed by any of the authors.

REFERENCES

[1]Abi Abdallah, D., A. Drochon, V. Robin, and O. Fokapu. Effects of static magnetic field exposure on blood flow. *Eur Phys J Appl Phys* 45:11301, 2009.

[2]Barnothy, M. F. Biological Effects of Magnetic Fields. Volume 1 and 2, Plenum Press, New York, 1964–1969.

[3]Caro, C. G., J. M. Fitz-Gerald, and R. C. Schroter. Atheroma and arterial wall shear observation, correlation and proposal of a shear dependent mass transfer mechanism for atherogenesis. *Proc R Soc Lond B* 177:109–159, 1971.

[4]Chaturani, P., and S. S. Bharatiya. Two layered magnetohydrodynamic flow through parallel plates with applications. *Indian J. Pure Appl. Math.* 32(1):55–68, 2001.

[5]Cheng, C., F. Helderman, D. Tempel, and D. Segers. Review: large variations in absolute wall shear stress levels within one species and between species. *Atherosclerosis.* 195:225–235, 2007.

[6]Committee on Opportunities in High Magnetic Field Science, Solid State Sciences Committee, Board on Physics and Astronomy Division on Engineering and Physical Sciences National Research Council of the National Academies, Opportunities in High Magnetic Field Science, The National Academies Press, Washington, DC, 2005.

[7]Cosmus, T. C., and M. Parizh. Advances in whole body MRI magnets. *IEEE Trans Appl Supercond* 21(3):2104–2109, 2011.

[8]Davies, P. F. Flow-mediated endothelial mechanotransduction. *Physiol Rev* 75:519–560, 1995.

[9]Formica, Domenico, and Sergio Silvestri. Biological effects of exposure to magnetic resonance imaging: an overview. *Biomed. Eng. Online.* 3:1–12, 2004.

[10]Fry, D. L. Certain chemorheologic considerations regarding the blood vascular interface with particular reference to coronary artery disease. *Circulation* 40:38–57, 1969.

[11]Gabe, I. T., J. H. Gault, J. Ross, D. T. Mason, C. J. Mills, J. P. Schillingford, and E. Braunwald. Measurement of instantaneous blood flow velocity and pressure in conscious man with a catheter-tip velocity probe. *Circulation* 40:603–614, 1969.

[12]Gabriel, S., R. W. Lau, and C. Gabriel. The dielectric properties of biological tissues: III. Parametric models for the dielectric spectrum of tissues. *Phys Med Biol* 41:2271–2293, 1996.

[13]Gayathri, K., and K. Shailendhra. Pulsatile blood flow in large arteries: a comparative study of Burton's and McDonald's models. *Appl. Math. Mech. Engl.* 35:575–590, 2014.

[14]Gayathri, K., and K. Shailendhra. Mathematical investigation of aetiology and pathogensis of atherosclerosis in human arteries. *Int J Bioinform Res Appl* 14:3–28, 2018.

[15]Gayathri, K., and K. Shailendhra. A mathematical modelling on the effect of high intensity magnetic fields on pulsatile blood flow in human arteries. *Int. J. Bioinform. Res. Appl.* 14:70–89, 2018.

[16]Geva, Tal. Magnetic resonance imaging: historical perspective. *J. Cardiovasc. Magn.* 8:573–580, 2006.

[17]Harvey, P. R., J. A. Overweg, C. Leonardus, G. Ham, N. B. Roozen, and P. W. P. Limpens. Open MRI magnet system, US7193416B2, 2007.

[18]He, X., and D. N. Ku. Pulsatile flow in the human left coronary artery bifurcation: average conditions. *J Biomech Eng* 118:74–82, 1996.
[19]Himburg, H. A., D. M. Grzybowski, A. L. Hazel, J. A. LaMack, Xue-Mei Li, and M. H. Friedman. Spatial comparison between wall shear stress measures and porcine arterial endothelial permeability. *Am. J. Physiol. Heart Circ. Physiol.* 286:H1916–H1922, 2004.
[20]Kangarlu, A., R. E. Burgess, H. Zhu, T. Nakayama, R. L. Hamlin, A. M. Abduljalil, and P. M. L. Robitaille. Cognitive, cardiac, and physiological safety studies in ultra high field magnetic resonance imaging. *Magn Reson Imaging* 17:1407–1416, 1999.
[21]Keltner, J. R., M. S. Roos, P. R. Brakeman, and T. F. Budinger. Magnetohydrodynamics of blood flow. *Magn Reson Med* 16:139–149, 1990.
[22]Kolin, A. An electromagnetic flowmeter: principle of method and its application to blood flow measurements. *Exp. Biol. Med.* 35:53–56, 1936.
[23]Korchevskii, E. M., and L. S. Marcochnik. Magnetohydrodynaic version of movement of blood. *Biophysics.* 10:411–413, 1965.
[24]Kornet, L., A. P. Hoeks, J. Lambregts, and R. S. Reneman. Mean wall shear stress in the femoral arterial bifurcation is low and independent of age at rest. *J Vasc Res* 37:112–122, 2000.
[25]Lee, S., L. Antiga, and D. A. Steinman. Correlations among indicators of disturbed flow at the normal carotid bifurcation. *J Biomech Eng* 131:061013–1–061013-7, 2009.
[26]Malek, A. M., S. Alper, and S. Izumo. Hemodynamic shear stress and its role in atherosclerosis. *J. Am. Med. Assoc.* 282:2035–2042, 1999.
[27]McKay, J. C., F. S. Prato, and A. W. Thomas. A literature review: the effects of magnetic field exposure on blood flow and blood vessels in the microvasculature. *Bioelectromagnetics.* 28:81–98, 2007.
[28]Nichols, W. W., and M. F. O'Rourke. McDonald's Blood Flow in Arteries, Theoretical, Experimental and Clinical Principles (5th ed.). New York: Oxford University Press, 2005.
[29]Novak, V. A. M., P. Novak Abduljalil, and P. M. Robitaille. High-resolution ultrahigh-field MRI of stroke. *Magn Reson Imaging* 23:539–548, 2005.
[30]Ofili, E. O., M. J. Kern, A. J. Labovitz, J. A. S. T. Vrain, J. Segal, F. V. Aguirre, and R. Castello. Analysis of coronary blood flow velocity dynamics in angiographically normal and stenosed arteries before and after endolumen enlargement by angioplasty. *J Am Coll Cardiol* 21:308–316, 1993.
[31]Schenck, J. F. Safety of strong, static magnetic fields. *J Magn Reson Imaging* 12:2–19, 2000.
[32]Shoemaker, J. K., S. M. Phillips, H. J. Green, and R. L. Hughson. Faster femoral artery blood velocity kinetics at the onset of exercise following short-term training. *Cardiovasc Res* 31:278–286, 1996.
[33]Shukla, J. B., R. S. Parihar, and B. R. P. Rao. Effect of stenosis on non-Newtonian flow of the blood in an artery. *Bull Math Biol* 42:283–294, 1980.
[34]Sinoway, L. I., C. Hendrickson, W. R. Davidson, S. Prophet, and R. Zelis. Characteristics of flow-mediated brachial artery vasodilation in human subjects. *Circ Res* 64:32–42, 1989.
[35]Tang, B. T., S. S. Pickard, F. P. Chan, P. S. Tsao, C. A. Taylor, and J. A. Feinstein. Wall shear stress is decreased in the pulmonary arteries of patients with pulmonary arterial hypertension: An image-based, computational fluid dynamics study. *Pulm. Circ.* 2:470–476, 2012.
[36]Terada, M., Yasuo Takehara, Haruo Isoda, Tomohiro Uto, Masaki Matsunaga, and Marcus Alley. Low WSS high OSI measured by 3D Cine PC MRI reflect high pulmonary artery pressures in suspected secondary pulmonary arterial hypertension. *Magn. Reson. Med. Sci.* 15:193–202, 2016.
[37]Thosar, S. S., S. L. Bielko, C. C. Wiggins, and J. P. Wallace. Differences in brachial and femoral artery responses to prolonged sitting. *Cardiovasc. Ultrasound* 12:50, 2014.
[38]Tzirtzilakis, E. E. A mathematical model for blood flow in magnetic field. *Phys Fluids* 17:077103–1–077103-15, 2005.
[39]Ugurbil, K., G. Adriany, P. Andersen, W. Chen, M. Garwood, R. Gruetter, P.-G. Henry, S.-G. Kim, H. Lieu, I. Tkac, T. Vaughan, P.-F. Van De Moortele, E. Yacoub, and X.-H. Zhu. Ultrahigh field magnetic resonance imaging and spectroscopy. *Magn Reson Imaging* 21:1263–1281, 2003.
[40]Verbeke, F. H., M. Agharazii, P. Boutouyrie, B. Pannier, A. P. Guenin, and G. M. London. Local shear stress and brachial artery functions in end-stage renal disease. *J Am Soc Nephrol* 18:621–628, 2007.
[41]Vinod, T., R. K. Purushothaman, K. Shailendhra, and Gayathri K. Pulsatile blood flow in large arteries with BJR slip condition. In: International Conference on Electrical, Electronics, and Optimization Techniques (ICEEOT-2016). 1700–1705, 2016.
[42]Whale, M. D., A. J. Grodzinsky, and M. Johnson. The effect of aging and pressure on the specific hydraulic conductivity of the aortic wall. *Biorheology* 33:17–44, 1996.

Publisher's Note Springer Nature remains neutral with regard to jurisdictional claims in published maps and institutional affiliations.